

# Microstructural analysis of the fractured railway freight car axle



**Z. Odanović**



**IMS Institute, Bulevar vojvode Mišića 43,  
Belgrade, Serbia**

# INTRODUCTION

- *Railway axles are designed to be highly reliable, while the maintenance system requires periodically inspection.*
- *Due to complex exploitation conditions, complex stress state and multiple stress concentration, railway axles could suffer fatigue failures.*
- *This investigation presents an attempt to clarify causes of the axle fracture of railway freight car for coal transport in a thermal power plant.*
- *Detailed analyses were conducted on the axle*
  - *mechanical properties,*
  - *failure analysis of the fractured surface in axle cross section,*
  - *macro and microstructure of the axle material.*

# EXPERIMENTAL

In order to identify the cause of axle fracture, following analyses and activities have been undertaken on the axle material :

- **Visual examination**
- **Chemical composition analyses**
- **Mechanical properties testing**
  - tensile testing
  - impact energy
  - plane strain fracture toughness  $K_{Ic}$  is estimated
  - hardness
- **Metallographic investigations**
  - macrostructural
    - fractured surface analysis
    - macroscopic method using sulphur print (Baumann method).
  - microstructural investigations were conducted using
    - Light Optical Microscopy (LOM)
    - Scanning Electron Microscopy (SEM)
    - Energy Dispersive X-ray analysis (EDX)

# RESULTS AND DISCUSSION

## *Visual examination*



**Fig. 1. Damaged railway freight car**

**Axle fracture occurred in the cross-section located between the roller bearing and railway wheel on the transition radius**



**Fig. 2. The railway wheel and axle with signed fractured surface**



**Fig. 3. Journal on the side of the railway axle where fracture has not occurred**

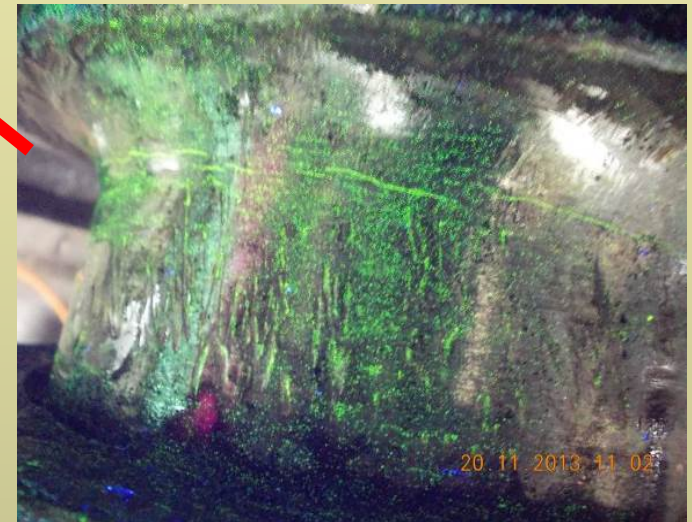


**Fig. 4. Appearance of cracks registered at the source of the stress concentration**

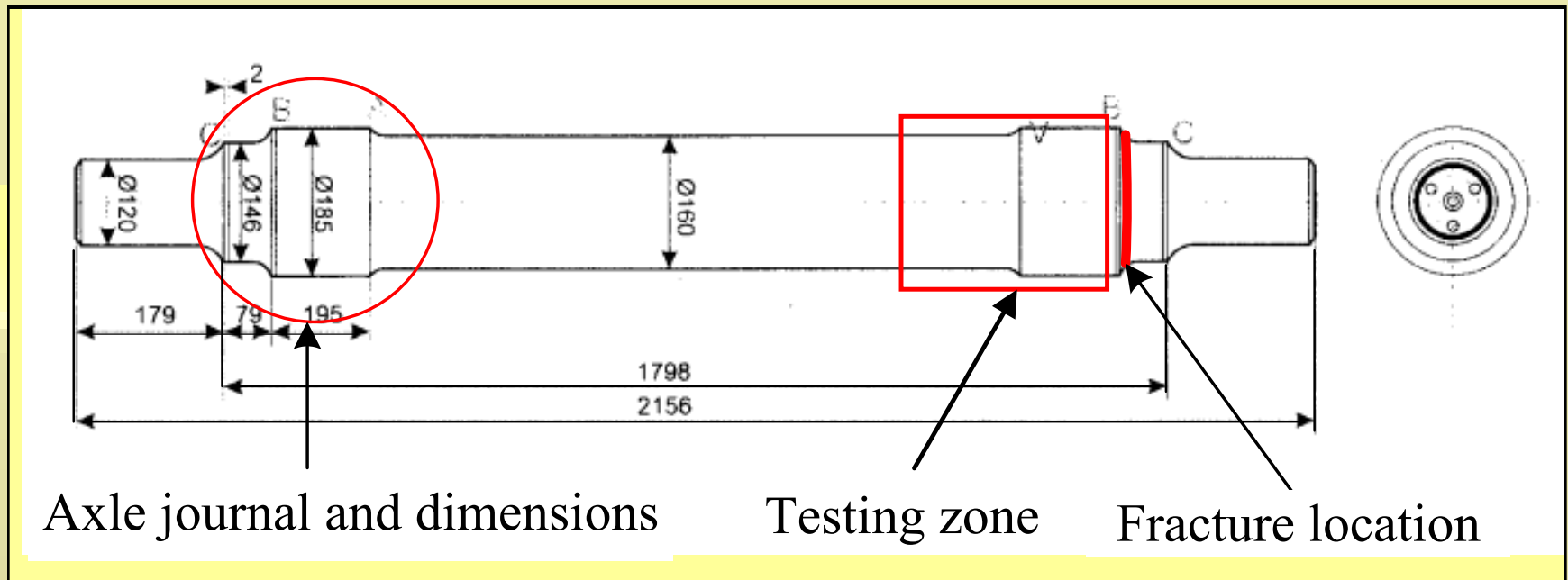


**Fig. 3. Details of the investigated railway axle,**  
 — geometry and dimensions in mm,  
 — fracture location,  
 — tested zone

- Axle was designed and manufactured 35 years ago, according to the national standard SRPS P.F2.310 (now similar to EN 13261:2003).
- Investigated axle was manufactured as solid and coated axle.
- Available user's data show that similar axle fractures were not recorded before
- The railway axle is regularly periodically inspected.

## *Chemical composition analysis*

**Table 1. Results of the axle material chemical analysis (mass. %)**

| Chemical element<br>(mass. %) | C            | Si           | S             | P             | Mn           | Ni           | Cr           | Mo           | V            | Ti     | W     | Al    | Fe   |
|-------------------------------|--------------|--------------|---------------|---------------|--------------|--------------|--------------|--------------|--------------|--------|-------|-------|------|
| Sample contents               | 0.441        | 0.260        | 0.005         | 0.009         | 0.640        | 0.034        | 0.097        | 0.012        | <0.003       | <0.003 | 0.020 | 0.069 | rest |
| Standard EN 13261             | max.<br>0.40 | max.<br>0.50 | max.<br>0.020 | max.<br>0.020 | max.<br>1.20 | max.<br>0.30 | max.<br>0.30 | max.<br>0.08 | max.<br>0.06 | -      | -     | -     | rest |
| Standard SRPS<br>P.F2.310     | ND*          | max.<br>0.50 | max.<br>0.05  | max.<br>0.05  | max.<br>1.20 | max.<br>0.20 | max.<br>0.30 | max.<br>0.05 | max.<br>0.05 |        |       |       | rest |

## *Mechanical properties*

**Table 2. Results of the tensile properties**

| Test specimens position                              | Yield Strength<br>$R_e$ (MPa) | Tensile Strength<br>$R_m$ (MPa) | Elongation<br>$A_5$ (%) | Contraction<br>$Z$ (%) |
|--|-------------------------------|---------------------------------|-------------------------|------------------------|
| Longitudinal   | 235                           | 534                             | 30.70                   | 51.58                  |
| Transverse   | 233                           | 523                             | 16.25                   | 17.86                  |
| Standard EN 13261<br>for longitudinal direction      | min 320                       | 550 - 650                       | min 22                  | /                      |
| Standard SRPS P.F2.310<br>for longitudinal direction | /                             | 550 - 630                       | /                       | /                      |

**Table 3. Impact energy results**

| <b>Test specimens position</b> | <b>Test temp. T(°C)</b> | <b>Middle value KU<sub>5/300</sub> (J)</b> | <b>Standard EN 13261 KU<sub>5/300</sub> (J)</b> |
|--------------------------------|-------------------------|--|---|
| <b>Longitudinal</b>            | <b>+ 20</b>             | <b>21.8</b>                                | <b>min. 30</b>                                  |
| <b>Transverse</b>              | <b>+ 20</b>             | <b>11.33</b>                               | <b>min. 25</b>                                  |

**Table 4. Measured material hardness through the axle cross section**

| <b>Measured hardness (HBW)</b>     | <b>Middle value (HBW)</b> |
|------------------------------------|---------------------------|
| <b>Surface: 146 – 148 – 149</b>    | <b>145.3</b>              |
| <b>Mid-radius: 145 – 145 – 144</b> |                           |
| <b>Centre: 143 – 145 - 143</b>     |                           |



# *Fracture mechanics parameter - strain fracture toughness $K_{Ic}$ – estimation*

In order to anticipate the ability of the tested steel to resist crack propagation, the fracture mechanics parameter - plane strain fracture toughness  $K_{Ic}$  is estimated from the measured values:

- yield strength and
- impact energy

Estimation was based on the Barsom-Rolfe correlation model:

$$K_{Ic}^2 \text{ [ksi.in}^{0.5}] = 5 * CVN * \sigma_{ys} - 0.25 * \sigma_{ys}^2 \dots\dots\dots (1)$$

$$K_{Ic}^2 \text{ [MPa.m}^{0.5}] = 0.619 * KV * Re - 0.00578 * Re^2 \dots\dots\dots (2)$$

$$K_{Ic}^2 \text{ [MPa.m}^{0.5}] = 0.27236 * KU * Re - 0.00578 * Re^2 \dots\dots\dots (3)$$

**Table 5. Calculated plane strain fracture toughness  $K_{Ic}$**

| Test specimens position | Impact energy $KU_{5/300}$ (J) | Yield Strength, $R_e$ (MPa) |                 | Strain fracture toughness $K_{Ic}$ (MPa.m <sup>0.5</sup> ) |
|-------------------------|--------------------------------|-----------------------------|-----------------|--|
| Longitudinal            | min. 30                        | min 320                     | <b>Standard</b> | 44.97  |
| Transverse              | min. 25                        |                             | <b>EN 13261</b> | 39.83  |
| Longitudinal            | 21.8                           | 235                         | <b>Measured</b> | 32.80  |
| Transverse              | 11.33                          | 233                         | <b>values</b>   | 20.13  |

# Macro and microstructure analysis of the fractured railway axle

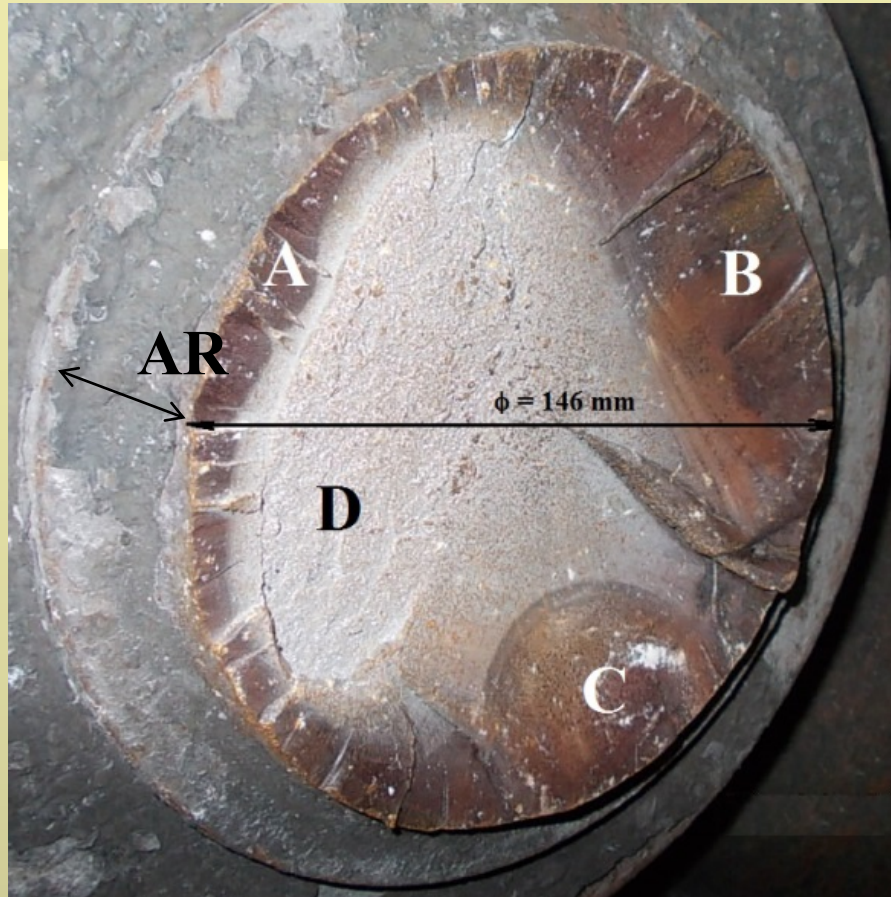


Fig. 4. Fractured axle surface

## A zone

- Numerous initial cracks on the outer surface of the *critical axle radius AR*.
- Spread parallel to the axle cross section.
- Formed specific shape of *tooth like initial cracks*.
- Presence of corrosion was evidenced.

## B and C zone

- Similar in morphology, but different in shape.
- Initialised at the ratchet marks and propagated by the *fatigue mechanism*.
- Highly oxidised which indicates long presence in axle exploitation.

## D zone

- Final axle fracture, *ductile* in morphology accounts for approx. 30 – 40% of the cross-sectional area.

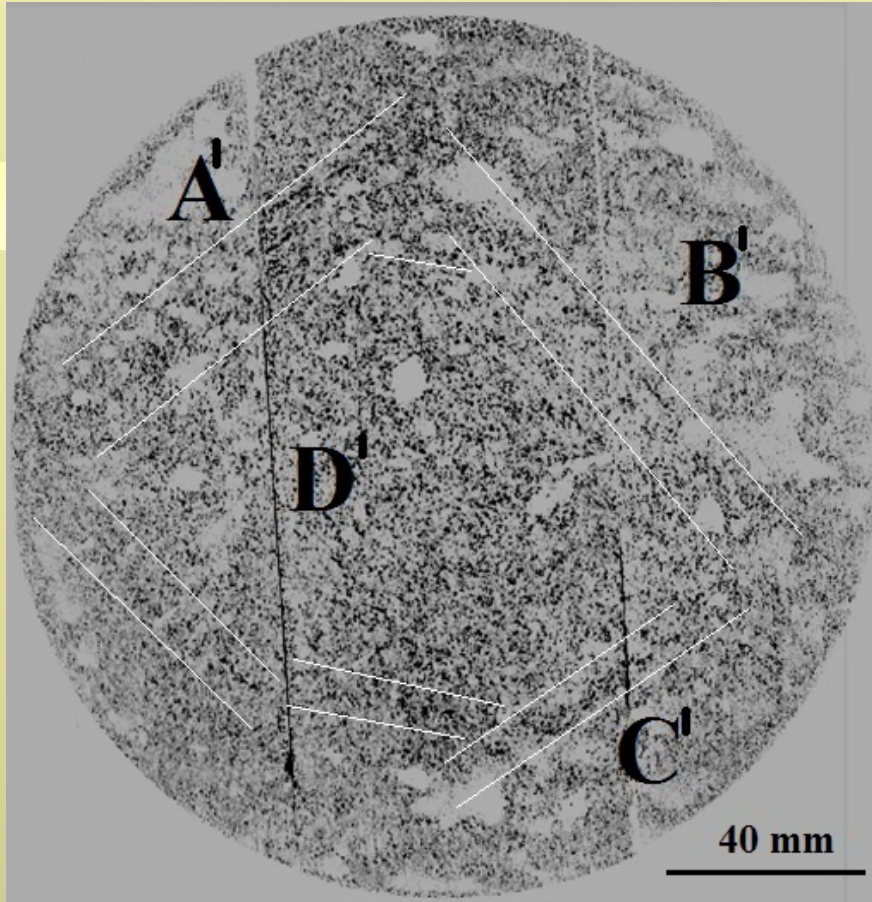


**Fig. 5. Macrostructure of the axle cross section obtained by sulphur print (Baumann method)**

- Small-scale heterogeneities in the central zone of the cross section.
- Dark etching *strings of inclusion* between the marked white lines at the mid radius.
- Comparing, one could notice matching between zones signed as A'-B'-C'-D' and A-B-C-D from Fig.4.

**It could be supposed:**

- Initial cracks from the axle surface were propagated through the cross section in the transversal direction, until reaching the strings of inclusions in zone between white lines.
- Orientation of these inclusion is perpendicular to the direction of the cracks propagation, and it could be assumed that represents *barrier* to the further crack propagation in radial direction for some period.

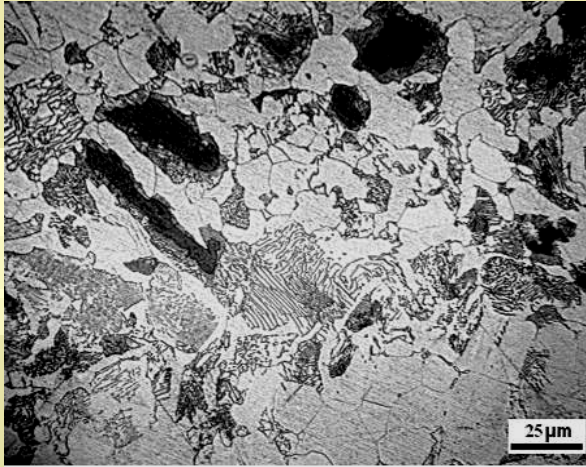
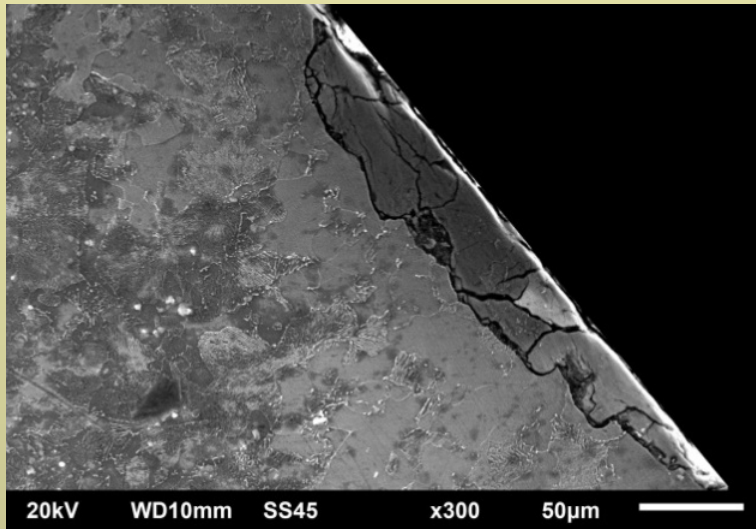
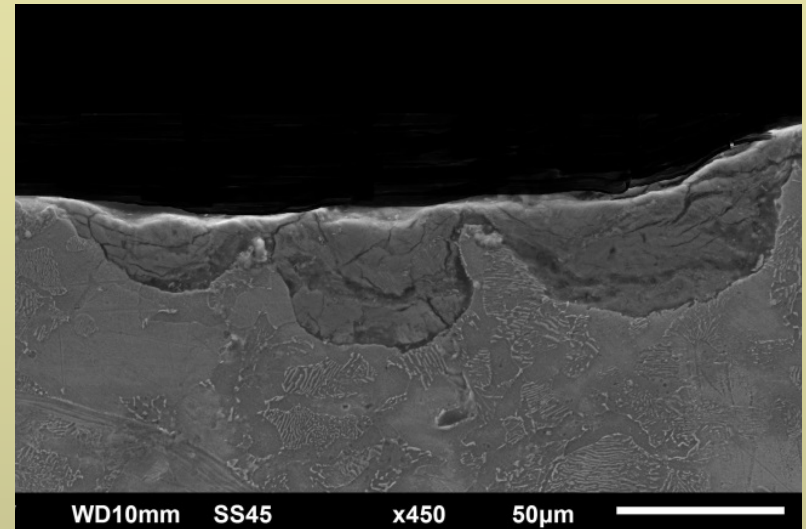


**Fig. 6. Lamellar perlite and ferrite in the axle material microstructure (etched in 3 % Nital)**

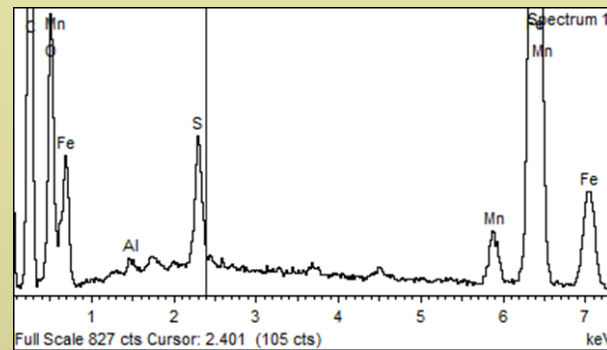
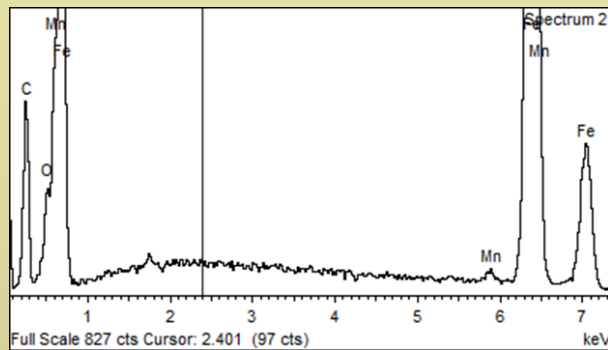
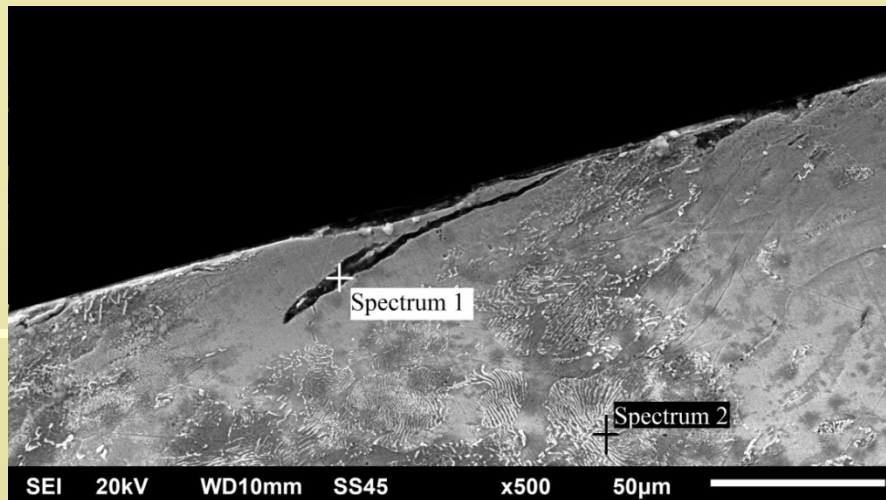


**a) wide, shallow**



**b) elliptical**

**Fig. 7. Corrosion pits in the axle material surface layer in the transition radius zone AR**



| Element | Weight, % | Atomic, % | Element | Weight, % | Atomic, % |
|---------|-----------|-----------|---------|-----------|-----------|
| C K     | 37.69     | 63.14     | C K     | 23.17     | 55.22     |
| O K     | 15.41     | 19.38     | O K     | 4.23      | 7.57      |
| Al K    | 0.22      | 0.16      | Mn K    | 0.50      | 0.26      |
| S K     | 1.81      | 1.14      | Fe K    | 72.09     | 36.95     |
| Mn K    | 2.27      | 0.83      | Totals  | 100.00    |           |
| Fe K    | 42.60     | 15.35     |         |           |           |
| Totals  | 100.00    |           |         |           |           |

**Fig. 8. Corrosion damage in the material surface layer with subjoined non-metallic inclusions located in a ferritic band**

# CONCLUSIONS

Based on the results obtained from the performed investigations, the following conclusions could be made:

- ✓ The results obtained from chemical composition testing indicate that the applied steel used for this type of axles is in accordance with the requirements of the relevant standards.
- ✓ Mechanical properties of applied material are below the standard requirements.
- ✓ Estimated low values of the strain fracture toughness  $K_{Ic}$ , especially in transverse direction, indicate low resistivity to crack propagation of the crack initials from the axle surface.
- ✓ Low values of the tested mechanical properties could be explained as a result of the inadequately applied reduction rate in hot rolling/forging process during the axle production, or inadequately applied heat treatment process.

# CONCLUSIONS

- ✓ It can be concluded that corrosion was initiated from the locations of damaged axle coat, and from below the coat to the whole surface of the critical radius thus creating conditions for pits forming.
- ✓ Crack initials are caused by corrosion pits at the surface of the critical radius of the axle.
- ✓ Due to the weakness of the material these cracks propagated, connected and spread by fatigue mechanism, until the axle cross-section could not to confront to the stresses arised from exploitation conditions.
- ✓ These circumstances lead to final fracture of axle.
- ✓ In order to prevent the reappearance of resulting damage, it is necessary to improve the control of the corrosion protection and the inspection of the axle from the aspect of the initial cracks during the regular maintenance.





**Thank you for your attention !**